

Results: Figure-1 shows a spatial normalization example and a mean BV/TV map. Cortical thickness maps of a scan-rescan example, mean cortical thickness maps, and a laminar vBMD example are shown in Figure-2. No significantly different voxels or vertices were found after FDR correction, indicating no significant multi-parametric differences between “baseline” and “follow-up” scans. Global reproducibility yielded CVRMS of 1.6% (0.018mm) and 0.9% (0.013mm) for apparent thickness, 1.5% (0.014mm) and 0.9% (0.010mm) for SIT, and 1.2% (4.68mg/cm³) and 0.8% (3.05mg/cm³) for vBMD, for the radius and tibia, respectively.

Conclusion: Advanced 3D image analysis techniques may be employed for population-based local multi-parametric comparisons of HR-pQCT studies with high reproducibility.

Acknowledgments

NIH-NIAMS: R01AR064140-R01AR060700.

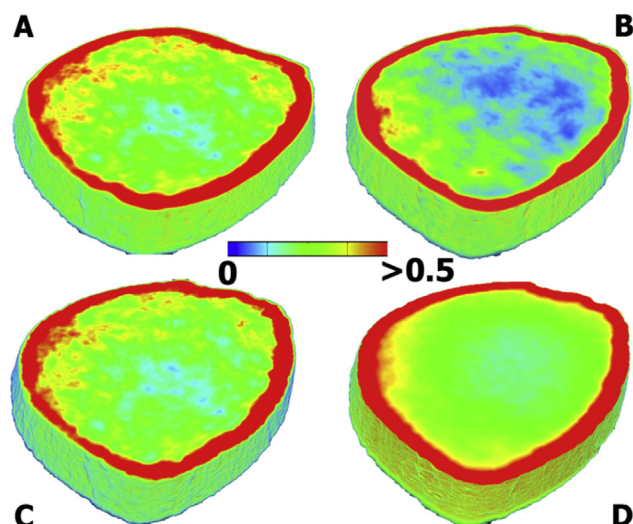


Figure 1. Cross-sections of voxel-wise analyses: A) Representative homogenized BV/TV map. B) Reference shape. C) Map in A after spatial normalization to B. D) Mean “baseline” BV/TV map.

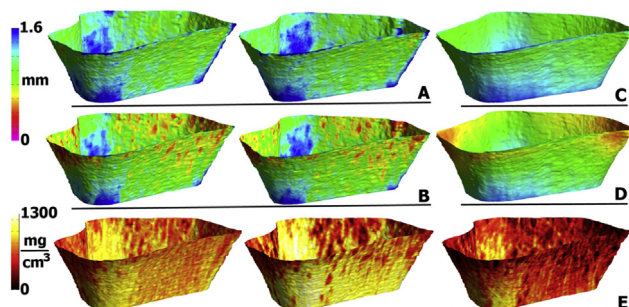


Figure 2. Surface-based analysis: A) Representative “baseline” and “follow-up” apparent cortical bone thickness maps. B) Representative “baseline” and “follow-up” SIT maps. C) Mean apparent cortical bone thickness map. D) Mean SIT map. E) Representative laminar vBMD maps: periosteal layer, middle layer, and endosteal layer.

IBDW2014-00138-F0061

HIGH RESOLUTION COMPUTED RADIOGRAPHY OF CORTICAL BONE POROSITY IN WEIGHT BEARING AND NON-WEIGHT BEARING LONG BONE SHAFT UNDER HABITUAL LOADING

Chung Ning Lam ^a, Yau Ming Lai ^a, Vivian Wing Ying Hung ^b, Ling Qin ^b

^aDepartment of Health Technology and Informatics, The Hong Kong Polytechnic University, HKSAR, PR China

^bDepartment of Orthopaedics and Traumatology, The Chinese University of Hong Kong, HKSAR, PR China

Objective: Differential mechanical loading in weight bearing and non-weight bearing long bone could result in adaptation of bone mineral density and microarchitecture. Understanding of the bone adaptation could shed light into the bone remodelling processes underpinning the adaptation. This study used high resolution computed radiography and post-image enhancement approach to quantify the intracortical porosity (ICP) of weight bearing and non-weight bearing long bone shafts under lifetime habitual loading at distal tibia and radius regions, respectively.

Methods: Cortical bone segments of 7.5 mm in length at distal tibia and radius were harvested from 20 Chinese cadavers aged 52 to 92. These were processed and embedded in methyl methacrylate (MMA) without decalcification. Bone slices of 500 μm were then cut from the MMA embedded bone specimens. Images of the bone slices were acquired using high resolution computed radiography with magnification technique. This rendered an in-plane resolution at 100 μm. Segmentation and quantification of cortical porosity from the mineralised tissues was achieved using Image J (National Institute of Health).

Results: The study demonstrated that tibial ICP (27.03 ± 2.93%) was 33% significantly higher than that of radius (20.37 ± 2.43%) (p < 0.001). The ICP correlated significantly with age, with radius showing strong correlation, r (17) = 0.75, p < 0.001, whereas tibia showing moderate correlation, r (18) = 0.44, p = 0.06. Two-way analysis of variance was carried out to study if there were any interaction effects of bone region (tibia and radius) and bone sector (anterior, posterior, medial, lateral cortices) on ICP. There was a marginally significant interaction between bone region and sector on ICP (p = 0.09). Follow-up test showed a marginally significant simple main effects for different sectors only in tibia (p = 0.03). The anterior cortex (28.26 ± 4.68 %) had 15% higher in ICP than the posterior cortex (24.55 ± 5.26 %) at the distal tibia (p = 0.003). No significant pairwise differences were found elsewhere.

Conclusion: It suggested that ICP increased with age because of unbalanced remodelling after mid-life. The high ICP in tibia may be a result of bone remodelling in response to dynamic loading so as to reduce the expenditure of mechanical energy for locomotion. Sectorial differences between the anterior and posterior cortex in distal tibia exemplified the bone adaptation to differential tension and compression strain mode, respectively.

IBDW2014-00139-F0062

ADVANCED MUSCULOSKELETAL IMAGING SYSTEMS ADOPTED FOR STUDY A NOVEL BONE-TARGETING DELIVERY SYSTEM CARRYING OSTEOPROMOTIVE PHYTOMOLECULE(S) DEVELOPED FOR PREVENTION OF ESTROGEN DEPLETION INDUCED OSTEOPOROSIS

Le Huang ^a, Xinluan Wang ^{a,c}, Nan Wang ^c, Heng Wu ^d, Jiayong Zhang ^b, Zhijun Yang ^b, Ling Qin ^{a,c}

^aMusculoskeletal Research Laboratory, Department of Orthopaedics and Traumatology, The Chinese University of Hong Kong, Hong Kong SAR, PR China

^bSchool of Chinese Medicine, Hong Kong Baptist University, Hong Kong SAR, PR China

^cTranslational Medicine R&D Center, Shenzhen Institutes of Advanced Technology Shenzhen, PR China

^dDepartment of Medicine, University of Minnesota, Minneapolis, USA

Objectives: To evaluate the efficacy of Icaritin with targeting liposome delivery system on prevention of estrogen depletion induced osteoporosis in vivo by analyzing the bone quality and microarchitecture by micro-Computed Tomography (micro-CT) and the distribution of the delivery system by using Xenogen IVIS spectrum system.

Methods: (ASP8)-Liposome-Icaritin was synthesized by thin film evaporation method with extruding through polycarbonate filter membranes to obtain unilamellar vesicles with bone targeting molecules ASP8 attached. Eighty four-month-old C57/BL6 female mice were divided into 8 groups (n=10): Baseline (BL), Sham surgery (SH), Ovariectomized (OVX), Estradiol for oral administration(O-E2), Icaritin for oral administration (O-ICT), low dose (8mg/kg, once a week) targeting delivery system with Icaritin injected via caudal vein (IV-LIP+ICT+ASP8-L), high dose (8mg/kg, twice a week) targeting delivery system with Icaritin injected via caudal vein (IV-LIP+ICT+ASP8-H), delivery system with Icaritin injected via caudal vein (IV-LIP+ICT, 8mg/kg, twice a week). Administrations of gavage and IV injection were applied respectively for 6 weeks from the day right after the OVX surgery. Lumbar spine and lower limbs were harvest 6 weeks after surgery for bone quality analysis. The 5th vertebra body of lumbar region was scanned by micro-CT (Scanco micro-CT 40). Trabecular bone was identified and parameters were analyzed for evaluation of bone quality and microarchitecture. For confirming the specificity of the targeting delivery system, Xenogen IVIS spectrum was used to semi-qualify the distribution of bone targeting system ex vivo by injecting labelled targeting delivery system.

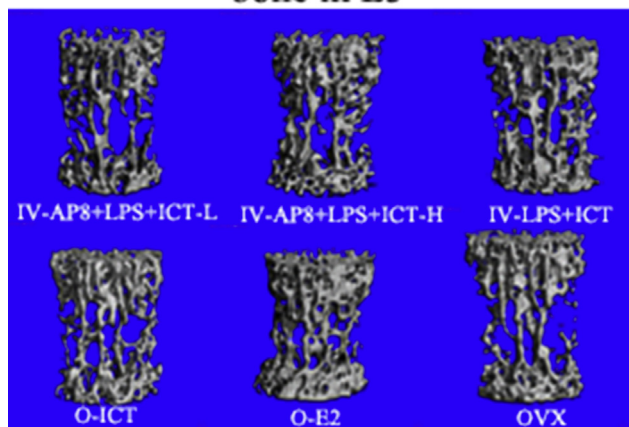
Results: By comparing to the OVX group, bone quality in groups with IV injection were enhanced reflected in the increased BMD ($p<0.05$), bone volume ($p<0.05$), trabecular bone number and connectivity density ($p<0.05$) and decreased in trabecular bone separation ($p<0.05$). Also the efficacy of the targeting icaritin delivery system tended to be dosage dependent (BV increased 14.16% in high dose group, Tb.N increased 10.34% and connectivity density of trabecular bone increased 19.70%). Moreover from Structure Model Index (SMI) value, we concluded that the morphology of trabecular bone in icaritin injection groups tends more to be plat-like: $SMI(OVX)=2.19\pm 0.30$, $SMI(IV-AP8+LPS+ICT-1)=2.07\pm 0.36$, $SMI(IV-AP8+LPS+ICT-H)=2.01\pm 0.23$. More signals retain in bone 72 hours after injection by comparing to the delivery system without bone targeting molecules ASP8 shown in IVIS image.

Conclusion: The novel bone-targeting delivery system carrying osteopromotive phytomolecule(s) Icaritin was confirmed that was capable of preventing the estrogen depletion induced osteoporosis in a dose dependent manner.

Acknowledgement: This study was supported by Hong Kong General Research Fund (GRF CUHK-473013).

Micro-CT 3D images of trabecular bone in L5.

Micro-CT 3D images of trabecular bone in L5



IBDW2014-00140-F0063

FRACTURE RISK OF ELDERLY POPULATION: LIKELIHOOD OF OSTEOPOROTIC FRACTURE RISK IN ELDERLY POPULATION AND INDOOR AIR POLLUTION

Xiaodong Pei^a, Zhiyi Huo^b, Lijun Pei^c

Department of Orthopedics, Fourth Hospital of Baotou, Inner Mongolia, China

^bDepartment of Medical Imaging, Haidian Hospital, Beijing, China

^cInstitute of Population Research, Peking University, Beijing, China

Background: Harmful particulate contaminants (such as PM_{2.5}) that indoor coal combustion produced can increase the incidence of cardiovascular disease and risk of death, while there is considerable evidence that cardiovascular disease, dyslipidemia, and osteoporosis among elderly population have common risk factors. Our hypothesis was that the osteoporotic fractures may be associated with indoor air pollution. The purpose of this study was to explore the risk of osteoporotic fracture of elderly population associated with likelihood of indoor air pollution.

Methods: Forty-eight cases with osteoporotic fractures and 91 controls were selected from the elderly population in Ordos region, Inner Mongolian. The risk factors were compared between the two groups in demographic characteristics, exercise, sleep, room environmental conditions, dietary, behavioral habits, history of medicine use, bone disease and chronic disease by using descriptive analysis. Multivariate logistic regression model was performed to analyze environmental risk factors associated with the risk of fractural etiology.

Results: The age range of case-control groups was 60-88 years old. There were no statistically significant differences between two groups in age, sex and occupation ($p>0.05$). The variables with statistically significant differences in the univariate analysis were included in Logistic Regression model. After adjustment for the education, ethnic factors, health status during childhood, behavioral habits, history of bone disease and medicine use, the findings showed that the exposure factors, such as indoor air conditions during the winter heating, weekly exercise, sleep quality, consumption of carbonated beverages, were associated with risk of elderly fracture. When compared to elderly population who had good air quality of habitable room in winter, elderly population with poor air quality had an elevated risk for fracture (OR 40.29, 95% CI 8.75-185.38); elderly population who had no weekly exercises had an increased risk for fracture (OR 4.28, 95% CI 1.20-15.24) when compared to those who had weekly exercises; elderly persons with poor quality of sleep was associated with a 6.85-fold increase in risk of fracture when compared to those with better quality of sleep (95% CI 1.61-29.14).

Conclusion: The findings suggest that poor indoor air quality during the winter heating may be the risk factors of osteoporotic fractures for the elderly population. It is necessary to further investigate those factors in a larger sample population.

IBDW2014-00141-F0064

EFFECT OF ANTHROPOMETRIC ADJUSTMENTS ON BMD AND BMC Z-SCORES IN A POPULATION OF PRADER-WILLI SYNDROME PEDIATRIC PATIENTS

Amanda E. Marker^a, David F. Short^a, Talia Eldar-Geva^b, Harry J. Hirsch^b, Varda Gross-Tsur^b, Maayan Tiomkin^c, Ari Zimran^c, Thomas N. Hangartner^a

^aBioMedical Imaging Laboratory, Wright State University, Dayton, OH USA

^bMulti-disciplinary PWS Clinic, Shaare Zedek Medical Center, Jerusalem, Israel

^cGaucher Clinic, Shaare Zedek Medical Center, Jerusalem, Israel

Objective: Two adjustment models were applied to a dataset of bone-mineral density (BMD) and bone-mineral content (BMC) from dual-energy x-ray absorptiometry (DXA) measurements of pediatric patients with Prader-Willi Syndrome (PWS). One model used weight, height and % body fat (WHF) in the calculation of Z-scores in addition to race, sex and age already included in the standard model. As percent body fat is not always available, a second model with only weight and height was also examined (WH).

Methods: Fifty-six patients with PWS, a neurogenetic disorder caused by the absence of paternal expression of imprinted genes localized in the 15q11-q13, were recruited. PWS is characterized by an insatiable appetite leading to obesity, short stature, cognitive and behavioral problems, hypogonadism and osteoporosis. All patients had spine and hip DXA measurements; 31/56 also had whole-body measurements (needed for body-fat correction). Several patients show lower than normal height or higher than normal weight for age. The percent body fat for all patients is either at the upper limit of or above the normal range. Patients with extreme anthropometric values were most affected by the anthropometrically corrected Z-scores.

Results: In the analysis of Z-scores, patients below -2.0, the critical region, are of most interest. By analyzing which patients cross the -2.0 boundary